Ceylon Journal of Science : Physical Sciences, 9(1), 1-8 (2002)

DYE- SENSITIZED SEMICONDUCTOR NANOSTRUCTURES FOR SOLAR ENERGY CONVERSION

KIRTHI TENNAKONE*

Institute of Fundamental Studies, Sri Lanka

ABSTRACT

Insight gained from experimental and theoretical studies on dye-sensitized solar cells made from different semiconductor materials and composites is summarized. Of the familiar high band gap oxide semiconductors TiO_2 based cells gives the highest recorded efficiency, short- circuit photocurrent and the open-circuit voltage. The reason for poor photovoltaic performance of SnO_2 is explained as trap mediated recombinations favored by low effective mass of electrons. However cells of efficiency comparable to TiO_2 could be fabricated from SnO_2 films coated with outer shells of insulators or high band gap semiconductors owing to confinement of electrons to the crystallites. It is argued that the fastness of transport of electrons in the nanocrystalline film again depends on the effective electron mass. Electron injection and motion in a dye- sensitized semiconductor nanowire is presented to illustrate how enhanced transport and suppression of the interaction of the conduction band electrons with acceptors may be achieved in a low dimensional dye-sensitized system.

1. INTRODUCTION

A photoexcited dye molecule anchored to a semiconductor surface could inject electrons to the conduction band at a rate even exceeding the vibrational relaxation. Fast injection, slow recombination of the injected electron with the dye-cation and the absence of positive holes in the semiconductor bulk are characters indicative of the utility of dye-sensitization for conversion of solar energy. The main problem in earlier attempts to devise dye-sensitized solar energy conversion systems had been their low energy and quantum conversion efficiency[1,3]. At monolayer or sub-monolayer coverage of the dye, the incident photons to photocurrent conversion efficiency per adsorbed dye molecule approaches unity. However in order to increase the energy conversion efficiency to a practically meaningful level, the light absorption cross section has to be increased by more than an order of magnitude. If the dye concentration is increased, several other factors which tend to decrease the efficiency are encountered. Thick dye layers, insulate electron conduction and also cut-off light that should be incident on the dye-molecules anchored to the semiconductor surface. Furthermore at higher surface concentrations of the dye, deactivation of excited dye molecules by mutual interaction (concentration quenching) is promoted. The above problems are elegantly resolved in the dye-sensitized (DS) nanocrystalline TiO_2 based solar cell developed by Gratzel and coworkers[4]. Here because of the high roughness factor (~ 1000) of the TiO_2 film, a monolayer coverage of the dye can be maintained while increasing the light absorption cross section nearly one thousand-fold. The optimized DS photoelectrochemical solar cells (PECs) made from nanocrystalline TiO_2 films have been reported to convert sunlight to electrical energy at an efficiency of ~ 10 % . Further improvement of the efficiency depends on finding ways of increasing the open-circuit voltage of the cell and broadening the spectral response. Open-circuit voltage depends on the quasi-fermi level of electrons in the semiconductor, which could rise up to the conduction band edge in the absence of recombinations. The

* tenna@ifs.ac.lk

recombinations of electrons with acceptors at the semiconductor/electrolyte interface limit the open-circuit voltage. An obvious way of broadening the spectral response would be the sensitization of the semiconductor film by a cocktail of dyes[5]. However, we then run into the following complication. As explained earlier, the overall dye-surface concentration will have to be maintained at the monolayer level thereby limiting the light absorption cross section corresponding to each dye. The loss in absorption cross section can be remedied only by increasing the film thickness (T), which should not greatly exceed the diffusion length $L_D = (D\tau)^{1/2}$, where D= diffusion coefficient of electrons and τ = recombination time. The diffusion coefficient depends on the material properties of the semiconductor and nature of the nanostructure. Thus an essential requirement for improvement of the efficiency of DS solar cells are strategies aimed at suppression of recombinations and enhancement of the dispersive transport of carriers in the semiconductor nanostructure. In this paper we give suggestions as to how the next generation of dye-sensitized solar cells may be modeled taking into consideration the above constraints.

2. EXPERIMENTAL

Fluorine doped conducting tin oxide glass plates (1.5x1 cm^2 , resistance ~ 15 ohm sq^{-1}) were used to deposit films of TiO_2 , SnO_2 and composites made from SnO_2 and other oxides. TiO_2 films were prepared by the method described in ref. 9. The following procedure was used to prepare films of SnO_2. Colloidal tin oxide (1ml, 15% aqueous dispersion, Alfa Aesar) is ground with few drops of glacial acetic acid , diluted to 75 ml and ultrasonically agitated for about 30 min after adding ~ 0.1ml of the surfactant Triton X 100. The dispersion is then sprayed onto conducting tin oxide glass plates heated ~ 150° C and sintered in air at 550°C for 30 mins. SnO_2 films where the crystallites are covered with a thin shell of MgO, ZnO or Al_2O_3 were made by incorporating the appropriate amount of MgO , ZnO or Al $(OH)_3$ to the SnO_2 colloid before addition of acetic acid . An alternative method used for coating outer shells on crystallites was to boil the SnO_2 coated plates in a solution (~ 10^{-3} M) of the respective acetates in 90 % ethanol. Here oxide or hydrous oxide film gets deposited from hydrolysis of the metal acetate.

Plate is washed with ethanol and sintered at 400° C for 10 mins. Thickness of the films was determined by SEM. The average thickness of the outer shells on the SnO_2 crystallites were estimated by the method described below. Plates where the crystallites in the film are coated with outer shells are warmed in 0.5 HCl for several hours to dissolve the shell. The amount of metal in the solution is estimated by atomic absorption spectroscopy. Shell thickness (t) is calculated from the formula,

$$t = [\, W_o/(W_o + W_{SnO2})\,](\rho'/\rho_o)\,(T/R) \qquad (1)$$

where W_o = wt. of shell material , W_{SnO2} = wt. of SnO_2 , ρ_o = density of the shell material , ρ' = gross density of the film (determined from a knowledge of the weight, thickness and area of the film), T = film thickness and R = roughness factor of the film . Because of the extreme thinness of the outer shell ($\leq$ 1 nm) SEM or TEM did not resolve the outer shell on the crystallites. XRD measurements showed that composite oxides (SnO_2 and MgO, ZnO or Al_2O_3) were not formed during sintering at 550°C. EDX and XPS confirmed presence of the shell material and indicated that the shell thickness was in the nanometer to sub-nanometer range. Films deposited on conducting glass plates were coated with the dye cis-dithiocyanato[N-N'-bis(2,2'-bipyridyl-4,4'-dicarboxylic acid] Ru(II) by immersing the plates in a warm (~ 80°C) alcoholic solution (3X 10^{-3} M) of this dye for 4 h. The extent of dye adsorption was determined by desorbing the dye into an alcoholic solution of NaOH (5x 10^{-3}M) and spectrophotomeric estimation. The roughness factor of the films was calculated assuming that each dye molecule covered an area of 1 nm^2. PECs were fabricated by clamping the dyed film surface to the counterelectrode (lightly platinized conducting glass plate) and filling the capillary space between the plates with the electrolyte (0.6 dimethylpropyl imidazolium iodide + 0.1M LiI +0.05M I_2 + 0.5 M t- butylpyridine in methoxyacetonitrile). The I-V characteristics of the cells and the incident photon to photocurrent conversion efficiencies were recorded using a solar cell evaluation system (exposed cell area 0.25 cm^2). Photocurrent and photovoltage transients were

recorded with a home made set up, where a collimated white light beam from a halogen lamp is interposed by a fast (< 1 ms) mechanical shutter and the response was recorded on an oscilloscope.

3. RESULTS AND DISCUSSION

The material extensively used for experiments in dye-sensitization is TiO_2 and attempts to fabricate comparably efficient DS PECs from other familiar high band gap oxide materials (e.g., SnO_2, ZnO) has not been successful. However, the author of this paper and his collaborators have found that highly efficient DS PECs can be made from SnO_2 , provided the crystallites in the film are coated with an ultra thin shell of an insulator(MgO , Al_2O_3)or a high band gap semiconductor(ZnO)[6,7].The dramatic influence of the outer shell on performance of the cell is clearly evident from the values of short-circuit photocurrent (I_{sc}), open-circuit voltage (V_{oc}), efficiency (η) and fill-factor (FF) presented in Table.1 and the I-V curve of Fig.1.We also observed that the outer shells of same materials on TiO_2 crystallites did not have such favorable effect on the cell. The explanation we gave was that the rate of recombination of the injected electrons during their transport to the back contact depends on the effective mass of the carrier. Electrons injected to the conduction band , after relaxation enters into shallow traps and gets thermally re-emited back to the conduction band . The wave function of an electron in a shallow trap at a depth E below the bottom of the conduction band can be expressed as,

$$\Psi(r) = a^{-3/2} \pi^{1/2} \mathrm{Exp}(-r/a) \qquad (2)$$

where $a = \hbar /(2m^*E)^{1/2}$ and r = radial coordinate measured from the trapping site. When we set E = k_BT (T= room temperature) , we get a critical radius R_c for a semiconductor particle below which the electron wave function overlaps strongly with the 'out-side '. The critical radius R_c depends on the effective mass and therefore on nature of the material (i.e., R_c for SnO_2 and TiO_2 ~ 4 and 0.4 nm respectively). Electron leakage rate is ~ proportional to $N_t \mid \Psi \mid^2$ (N_t = density of trap sites) and recombination with an acceptor in the electrolyte (e.g., I_3^-) increases as the size of crystallites in the film is reduced and the effect should be noticeable in materials with sufficiently small effective mass. This indeed was verified when we examined DS PECs made SnO_2 films of different crystallite sizes. SnO_2 films made from commercially available SnO_2 colloidal solution (Alpha Chemicals) have crystallites of median size ~3 nm. We also prepared SnO_2 films having crystallites ~ 60 nm by hydrolysis of tin (iv) isopropoxide. Despite lower surface concentration of the dye, the values of V_{oc} (~530 mV), η(~ 2%) are higher in the cell with larger crystallites owing to the reduction in the recombination rate. The effect of N_t on recombinations becomes clearly evident when we construct DS PECs out of Sb-SnO_2 (antimony doped SnO_2) instead of SnO_2 . Here the ionized donors (N_t ~ 10^{21} cm^{-3}) act as trapping sites , greatly increasing the recombination rate.. A DS PEC made from a film of Sb-SnO_2 (crystallite size ~ 3 nm) was found to be inactive ($V_{oc} < 10^{-1}$ mV , $I_{sc} < 10^{-2}$ mA cm^{-2} at one sun). However when a thin layer of MgO was coated on Sb- SnO_2 crystallites V_{oc} , I_{sc} reached the values 475 mV , 7.3 mA cm^{-2} respectively (Table.1).

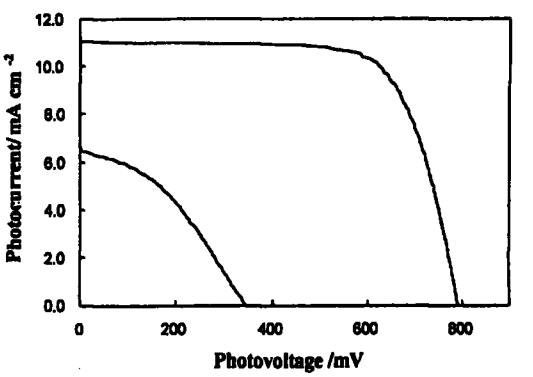

Fig. 1 I-V characteristics of a DS PEC made from (a) SnO_2 nanocrystalline film where the SnO_2 crystallites are coated with an MgO outer shell of thickness ~ 0.8 nm. and (b) SnO_2 film

The above experiments clearly demonstrate the effectiveness of an ultra-thin outer shell on SnO_2 crystallites in suppression of the recombinations. The optimum thickness of the shell was found to be ~ 0.8 nm (for MgO). Dye is anchored to the outer shell and the excited dye molecule injects electrons to the conduction band of SnO_2 tunneling across the barrier. Thicker barriers interfere with the electron injection process.

Table 1 Short-circuit photocurrent (I_{sc}), open-circuit voltage (V_{oc}) and fill factor (FF) of DS PECs made SnO_2, Sb-SnO_2 and TiO_2 where the respective crystallites are coated with different shell materials. The number within the brackets in the entries of the column 2 gives the shell thickness in nm.

Semiconductor	Shell	I_{sc}/mA cm^{-2}	V_{oc}/mV	η %	FF
SnO_2	-	6.6	345	0.86	0.37
SnO_2	MgO(0.8)	11	792	6.1	0. 73
SnO_2	ZnO (1.0)	16.8	650	6.9	0.65
SnO_2	Al_2O3 (1)	7.0	637	2.6	0.60
Sb-SnO_2	-	$< 10^{-2}$	10^{-1}	~ 0	-
Sb-SnO_2	MgO (0.8)	7.3	475	1.8	-
TiO_2	-	16.1	724	6.6	0.57
TiO_2	Al_2O_3	12.0	783	5.9	0.62

Table 2 Table showing the dependence of L_D (extrinsic Debye length), E_0 (ground state subband energy = subband spacing) and σ (extent of lateral spread of the ground state wave function) on material properties ε (dielectric constant) and N_D (doping density) of the nanowire

Material	ε	m^*/m_e	N_D /cm^3	L_D/nm	E_0/meV	σ /nm
GaAs	13	0. 07	10^{18}	19.4	7.4	9.9
GaAs	13	0.07	10^{19}	6.1	23.4	5.6
GaAs	13	0.07	10^{20}	1.94	74	3.3
SnO_2	10	0.1	10^{18}	17	5.1	14.6
SnO_2	10	0.1	10^{20}	1.7	51.4	4.6
Sb-SnO_2	10	0.1	10^{21}	0.5	115	2.6
TiO_2	100	10	10^{17}	168	0.7	14.6
TiO_2	100	10	10^{20}	5.3	22.1	2.6

Photocurrent and photovoltage transients of cells made from TiO_2 , SnO_2 , [SnO2]MgO (i.e., SnO_2 crystallites coated with a MgO shell) and [Sb-SnO_2]MgO are presented in Figs.2 and 3. The sharper response in [SnO_2] MgO compared to TiO_2 is a clear indication that the diffusion coefficient associated with dispersive transport is higher in [SnO_2]MgO. The diffusion coefficient of electrons in the nanocrystalline film is a gross factor depending on many parameters, i.e., (1) intrinsic diffusion coefficient of electrons in the semiconductor material, (2) composition of the electrolyte (i.e., ionic species present and the viscosity), (3) trapping and detrapping and (4) nature of tunneling of the electrons from one crystallite to the other. Intrinsic diffusion coefficient (D) is given by the relation D = μkT/e (mobility μ proportional to m^{*-1}). Therefore a lower effective mass favors fast transport. The tunneling probability of electrons from one crystallite to another across the neck region varies with effective mass as Exp[- $A(Bm^*)^{1/2}$] where A and B are constants. We believe that reason for faster transport in SnO_2 compared to TiO_2 originates from the above effects associated with smaller effective electron mass in SnO_2 (~ 0.1m_e [10-11]) compared to that in TiO_2 (10m_e [12] or 50m_e [13] according to some reports).

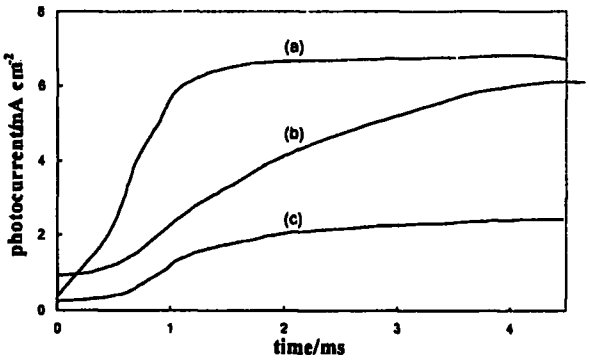

Fig. 2 Growth of short-circuit current (photo-current transient – light on) in dye-sensitized PECs made from (a) MgO coated SnO_2 (b) TiO_2 and (c) SnO_2 films

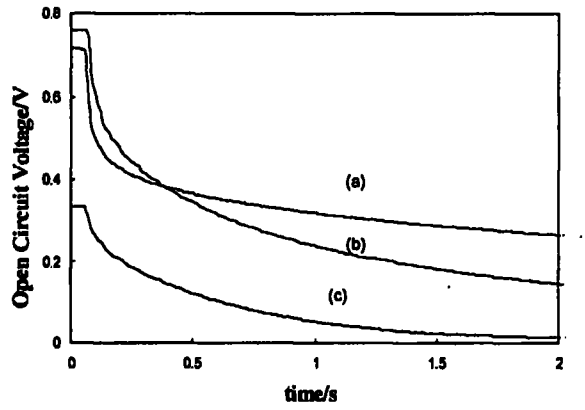

Fig. 3 Decay of open-circuit voltage (photo-voltage transient-light off) in a dye-sensitized PEC made from (a) MgO coated SnO_2 (b) TiO_2 (c) SnO_2 films

Question that arises is can the transport properties be further improved by modifications of the morphology of the film?. Nanocrystalline films used for DS solar cells thus far are aggregates of interconnected nanocrystallites. Necking between the crystallites and disorder slow down the transport. In order to gain understanding of the mechanism of electron transport and develop the next generation of DS PECS, it is instructive to consider dye-sensitization of semiconductor nanowires. Consider a wire of radius R made from a semiconductor material of dielectric constant ε doped to a donor density N_D. When the wire is surrounded by an electrolyte the flow of electrons to acceptors in the electrolyte generates a radial depletion field the extent of which is few times the extrinsic Debye length given by [14],

$$L_D = [\varepsilon kT/2e^2N_D]^{1/2} \qquad (3)$$

If $L_D \sim R$, the wire gets almost fully depleted (Fig.4) acquiring a charge volume density N_De and an electron placed at a distance r from the axis of the wire experiences a restoring force ,

$$\underline{F} = -[N_De^2/2]\,\underline{r} \qquad (4)$$

Thus the transverse motion is simple harmonic and the wave function of an electron in the wire can be written in cylindrical coordinates as,

$$\Psi(r,\theta,t) = \Phi(r,\theta)\,Exp[ikz - \omega t] \qquad (5)$$

where $\Phi(r,\theta)$ are the two dimensional simple harmonic oscillator eigenfunctions and second term in the product of (3) describes free particle motion in the z direction. The energy of the electron assumes the form,

$$E_{nm}(k) = h/2\pi\,[N_De^2/2m^*\varepsilon]^{1/2}(1+n+m) + h^2k^2/8\pi^2m^* \qquad (6)$$

where m^* = effective electron mass and the quantum numbers n,m define the subband energy level structure. When we write the ground state eigenfunction as,

$$\Phi_0(r) = [2^{1/2}/\pi\sigma]\,Exp(-r^2/\sigma^2) \qquad (7)$$

the parameter σ measuring the extent of spread of the ground state wave function is,

$$\sigma = [2\varepsilon h^2/m^*N_De^2]^{1/4} \qquad (8)$$

The conditions necessary for the practical realization of confinement by depletion are determined by the parameters L_D, E_0 [= E_{00} (k) = ground state energy = subband spacing] and σ. The condition $L_D \sim R$ needs to be satisfied in order to achieve full depletion (Fig.3). The subband quantum effects become observable when $E_0 > kT$. The confinement is possible according to the conditions assumed in the problem only if $R \geq \sigma$. It is important

to note the dependence of L_D, E_0 and σ on material properties of the wire, *i.e.*, dielectric constant, doping density and the effective electron mass [15]. Table.2 summarizes the values of these parameters for some selected materials. It is seen that for GaAs and SnO_2 quantum effects could manifest for practically meaningful wire sizes and doping densities at temperatures around the ambient. An advantage of using an electrolytic contact for achieving depletion is the ease with which a long delicate nanowire may be surrounded by a liquid to form a good contact compared to another solid. Solid to solid contact at nanoscale becomes more difficult and requires advanced fabrication methods. The virtue of confining the electrons to a ground state harmonic oscillator wave function (minimum uncertainty wave packet) is the very small probability of its interaction with the boundaries of the nanowire where recombinations and surface trapping are excessive. Thus transport along a nanowire surrounded by an electrolytic medium could be largely dissipationless and the transport could be ballistic[15]. Electron injection to a DS nanowire is equally important. The transition rate for electron injection in dye-sensitization is supposed to be described by a Fermi-Golden Rule type expression [16], $P = (4\pi^2/h) | H |^2 \rho$, where $| H |$ is the matrix element connecting the states in the excited dye molecule and the semiconductor and ρ is the density of final states in the semiconductor given by

$$\rho = 2/h [2m (E - E_{nm})]^{-½} \qquad (9)$$

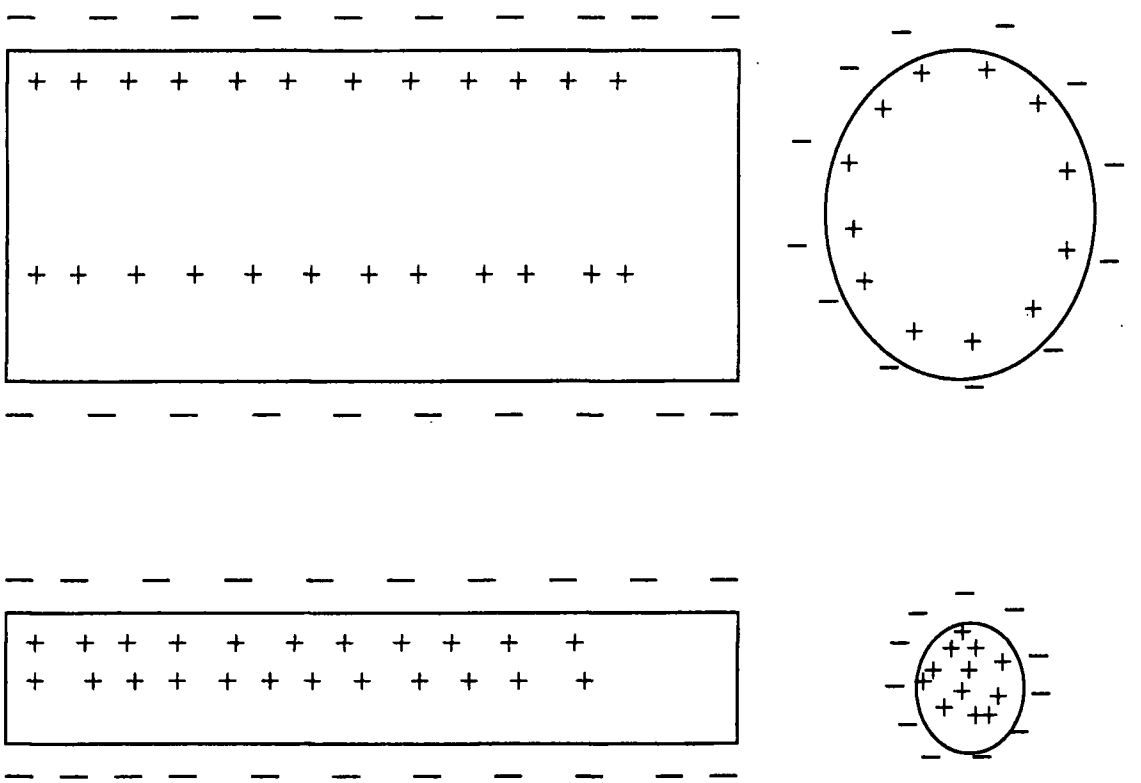

Fig. 4 Longitudinal sections and transverse of large ($R >> L_D$) and small ($R \sim L_D$) cylindrical wires showing depletion profiles developed upon immersion in an electrolyte.

As ρ tends become infinitely singular at a subband , the rate of electron injection to a subband would be exceedingly fast and therefore the probability of injection to any one of the subbands would be nearly the same (Fig.5) and the injection could be from any one of the vibrational levels in S^*. Thus rate of electron injection to a subband would supersede dissipative processes (i.e., back reactions, radiative deactivation, vibrational relaxation, concentration quenching *etc.*) encountered in dye-sensitization. The advantage is better utilization of hot carrier energy. A limitation to fast injection to subband followed by ballistic transport would be impurity scattering and trapping. As in nanocrystalline films, coating of the nanowire surface with an insulating shell would suppress trap mediated electron leakage.

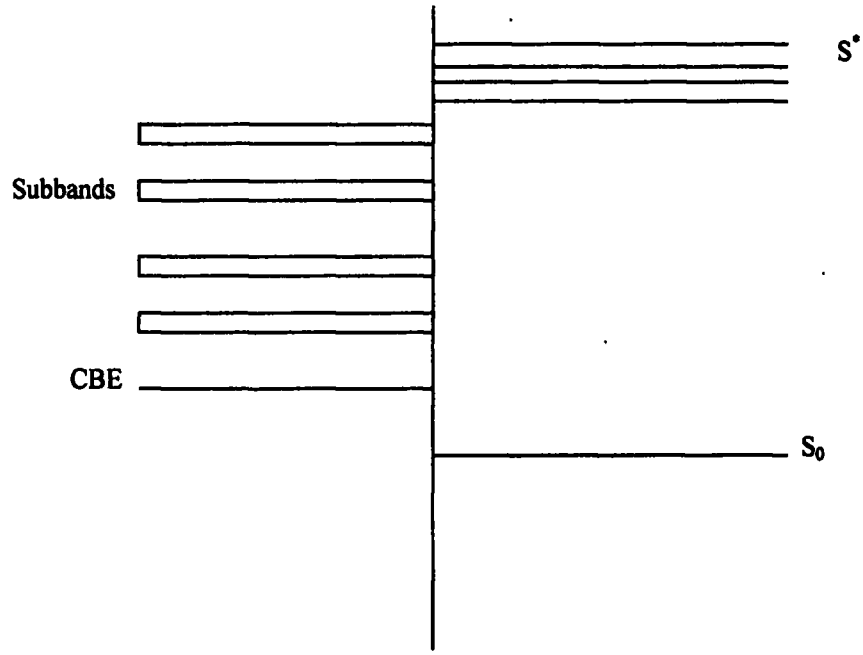

Fig. 5 A schematic energy level diagram showing the subbands of a nanowire, position of the conduction band edge (CBE) and ground (S_0) and excited (S^*) states of the dye molecule.

4. CONCLUSION

Our experiments suggest that electron transport in nanocrystalline SnO_2 films is faster than that in similar films made from TiO_2.The reason could be understood in terms of lower effective mass of electrons in SnO_2. Lower effective mass has the disadvantage as it promotes the rate of trap mediated recombinations and this can be circumvented by coating the SnO_2 crystallites surface with ultra thin shell of an insulator (e.g., MgO). SnO_2 also satisfies the criteria for electron confinement during transport in a nanowire surrounded by an electrolytic medium. If the problem of necking is reduced an interconnected chain of SnO_2 nanocrystallites would be a crude approximation to a nanowire. However, the effect of necking of crystallites, disorder and deviation from the straight-line paths would cause localization. Thus, improvement of the film morphology bringing in more order is an essential requirement enhancing the rate of transport. The effect of the electrolyte on the transport of electrons along the nanocrystallites is not fully understood. In the nanowire approximation confinement effectively screens electrons from outside effects. It is likely that effects of ionic species in the electrolyte on transport

become more prominent at the neck regions of a chain of interconnected nanocrystallites. Here R (wire radius) << σ and the conduction band states strongly interact with the electrolyte.

5. ACKNOWLEDGEMENTS

The author wishes to thank Mr. P.V.V. Jayaweera, Ms P.K.M Bandaranayake, Ms I.R.M.Kottegoda (Institute of Fundamental Studies, Sri esLanka) Dr. G.R.A.Kumara (Department of Materials Science, Shizuoka University, Hamamatsu, Japan), G.Kumarasinghe (Department of Physics, University of Birmingham, UK) for conducting some of the measurements reported in this paper.

REFERENCES

1. R.Memming, *Photochem.Photobiol* **16** (1972) 325.
2. M.Matsumura, Y.Nomura and H.Tsubomura, Bull. *Chem.Soc.Japan* **82** (1979) 1559.
3. H.Tsubomura, M.Matsumura , Y. Nomura and T . Amamia , *Nature* **261** 402.
4. B.O.Regan and M.Gratzel, *Nature* **353** (1991) 737.
5. K.Tennakone,G.K.R.Senadeera and P.V.V. Jayaweera , *Current Science* **81** (2001) 76.
6. K.Tennakone, J. Bandara, P.K.M. Bandaranayake, G.R.A.Kumara and A.Konno, *Jpn.J.Appl.Phy.* **40** (2001) L732.
7. K.Tennakone,V.P.S.Perera,I.R.M.Kottegoda,L.A. A.DE Silva, G.R.R.A. Kumara and A.Konno, *J.Electronic Materials* **30** (2001) 992.
8. G.R.A.A. Kumara, K.Tennakone, V.P.S. Perera,A. Konno ,S.Kaneko and M.Okuya, *J.Phys.D : Appl. Phys.* **34** (2001) 868.
9. M.K. Nazeerudin, A.Kay, I.Rodicio, R.Humphry Baker, E.Muller,P.Liska, N. Vlachopoulos and M.Gratzel , *J.Am.Chem.Soc.* **115** (1993) 6382.
10. D.F.Morgan and D.A. Wright, *Br.J.Appl.Phys.***17** (1996) 337.
11. R.Summitt and N.F. Borelli, J.Phys. *Chem.Solids* **26** (1965) 921.
12. C.Kormann, D.Bahnemann and M.Hoffmann, *J.Phys.*Chem.**92** (1988) 5196.
13. R.Breckenridge and W.Hosler, *Phys.Rev.* **91** (1953) 793.
14. S.M.Sze , *Physics of Semiconductor Devices* John Wiley (1981) 75.
15. K.Tennakone and P.V.V. Jayaweera (submitted for publication).
16. J.B.Asbury, E.Hao , Y.Wang , H.N. Gosh and T. Lain , *J. Phys. Chem.* B **105** (2001) 4545.